Cognitive Neurodynamics
https://doi.org/10.1007/s11571-021-09680-3

RESEARCH ARTICLE

Direction of information flow between brain regions in ADHD and healthy children based on EEG by using directed phase transfer entropy

Ali Ekhlasi[1] · Ali Motie Nasrabadi[2] · Mohammad Reza Mohammadi[3]

Received: 13 September 2020 / Revised: 4 April 2021 / Accepted: 16 April 2021

Abstract
Directed information flow between brain regions might be disrupted in children with Attention Deficit Hyperactivity Disorder (ADHD) which is related to the behavioral characteristics of ADHD. This paper aims to investigate the different information pathways of brain networks in children with ADHD in comparison with healthy subjects. EEG recordings were obtained from 61 children with ADHD and 60 healthy children without neurological disorders during attentional visual task. Effective connectivity among all scalp channels was calculated using directed phase transfer entropy (dPTE) for delta, theta, alpha, beta, and lower-gamma frequency bands. Group differences were evaluated using permutation tests in connectivity between regions. Significant posterior to anterior patterns of information flow in theta frequency bands were found in healthy subjects (*p-value* < 0.05), while disrupted pattern flow, in an opposite way, was found in ADHD children. In the beta band, information flow in pathways between anterior regions was significantly higher in healthy individuals than in the ADHD group. These differences are more indicated in connectivity that leads from frontal and central regions to the right frontal regions of the brain (F8 electrode). Furthermore, connections from central and lateral parietal areas to Pz electrode areas are statistically significant and higher in healthy children in this band. In the delta band, internal connections in the anterior region show a significant difference between the two groups, as this amount is higher in the ADHD group. Our analysis may provide new insights into information flow in brain regions of ADHD children in comparison with healthy children.

Keywords Electroencephalogram (EEG) · Effective Connectivity · Attention Deficit Hyperactivity Disorder (ADHD) · Directed Phase Transfer Entropy (dPTE)

Introduction

Attention Deficit Hyperactivity Disorder (ADHD) is a common childhood developmental disorder characterized by symptoms of inappropriate behavior, inattention, and/or hyperactivity and impulsivity. The prevalence of ADHD has been estimated at approximately 12.1% among boys and 3.9% among girls (Kessler et al., 2014). Since ADHD is considered a neurodevelopmental disorder beginning in childhood, early detection of this disorder is of great value (Kooij et al., 2010; Pub, 2013).

ADHD's behavior can be caused by differences in brain function. A method to elucidate these differences is to examine brain function with excellent temporal resolution, low-cost of data recording, and in a range of frequency bands, using electroencephalography (EEG) (González et al., 2017). Hitherto, much research has been conducted to distinguish differences between healthy and ADHD children using EEG signals. More basic research has shown ADHD patients have increased absolute and/or relative delta and theta power and decreased absolute and/or

✉ Ali Motie Nasrabadi
nasrabadi@shahed.ac.ir

1 Department of Biomedical Engineering, Science and Research Branch, Islamic Azad University, Tehran, Iran

2 Department of Biomedical Engineering, Faculty of Engineering, Shahed University, Tehran, Iran

3 Psychiatry and Psychology Research Center, Roozbeh Hospital, Tehran University of Medical Sciences, Tehran, Iran

relative beta and gamma power as compared to age-matched healthy controls, ordinarily recorded over fronto-focal electrodes, which are evaluated by the theta/beta ratio (TBR) (Barry and Clarke, 2013; Barry et al., 2003; Lenartowicz and Loo, 2014; Monastra, 2008). Based on the non-linear characteristics of EEG signals, several studies have used chaotic features to differentiate the patients from normal subjects (Allahverdy et al., 2016; Mohammadi et al., 2016).

EEG has been shown to be a reliable method for studying functional and effective connectivity of the brain in psychiatric disorders (Başar and Güntekin, 2013; van den Heuvel and Sporns, 2013). Previous studies of EEG connectivity in ADHD often calculated linear correlations between separate signals recorded on the scalp. These studies indicate ADHD subjects, compared to healthy controls, present higher intrahemispheric coherence in short/medium distances in delta, theta and beta frequency bands, reduced laterality in the theta band and increased frontal interhemispheric values in the delta and theta bands (Barry and Clarke, 2013; Barry et al., 2003; Clarke et al., 2007). Other studies have shown a specific deficit as a functional disconnection between frontal and occipital cortex in children with ADHD in a cross-model attention task (Mazaheri et al., 2010).

Both correlation and coherence are linear connectivity measures that are insensitive to nonlinear correlations (Vinck et al., 2011). Two measures, synchronization likelihood (SL), and fuzzy synchronization likelihood (FSL), were used to study the EEG connectivity of ADHD patients (Ahmadlou and Adeli, 2011a; b). The results demonstrated that the SL of the ADHD group was lower than that of the control group in posterior cortical areas at certain EEG bands. Moreover, ADHD subjects had a lower functional connectivity than the control group on the centerline of the brain, which could affect the communication between anterior and posterior lobes. van Diessen et al. (2015) proposed phase-based criteria (instead of amplitude) to eliminate the effect of volume conduction on the functional connectivity. Recently, Kiiski et al. (2020) reported functional EEG connectivity as a neuromarker for adult ADHD symptoms by calculating the weighted phase lag Index (WPLI) for each frequency band.

All previous studies used symmetric measures and did not consider the direction of information flows. Thus, effective connectivity, which deals with causal interactions of the brain regions, might provide more comprehensive information about the brain. A well-known effective connectivity measure that characterizes the information transfer between time series is transfer entropy (TE) (Schreiber, 2000). TE is a model-free connectivity measure that shows the direction of interactions and contains linear and nonlinear interaction based on information theory. TE is also extended on instantaneous phase data as phase transfer entropy (PTE). Therefore, this measure has two features, model-free and using phase, which may further overcome linear mixing and volume conduction respectively (Lobier et al., 2014). This criterion has also been used recently in the study of other signals such as magnetoencephalography (MEG) and in other diseases (Boon et al., 2017; Dauwan et al., 2016; Engels et al., 2017; Hasanzadeh et al., 2020; Hillebrand et al., 2016; Wang et al., 2019).

By using functional magnetic resonance imaging (fMRI), Rubia et al. (2010); (2009b) reported a reduced activation in the ADHD group in mesial and lateral prefrontal areas in the right hemisphere and in the cingulate gyrus. Booth et al. (2005) found that the ADHD group showed a decreased activation in a widespread network of frontal regions, predominantly in the right hemisphere. Furthermore, some studies provide evidence for reduced frontostriatal and frontoparietal functional connectivity in children with ADHD in the resting state (Kelly et al., 2007).

In the current study, it was hypothesized that the information flow in the brains of children with ADHD differs from that of healthy participants. Based on our knowledge, this study aimed to investigate the directed information and effective connectivity in ADHD patients with EEG by using dPTE in each frequency band during attentional task instead of resting state.

The rest of the paper has been categorized into four sections: within the" Methods" section, we describe the subjects of the study, EEG data recording and preprocessing, followed by the procedure of direction of information and statistical analysis between the two groups. In the "Results" section, obtained statistical differences are shown using the introduced criteria. The results are discussed and are compared to other research outcomes in the "Discussion" section. Finally, this paper is concluded in the "Conclusion" section.

Methods

Subjects

Participants were 61 children with ADHD (48 boys and 13 girls with a mean age of 9.62 ± 1.75 years old) and 60 healthy children (50 boys and 10 girls with a mean age of 9.85 ± 1.77 years old). Children with ADHD were diagnosed by an experienced child and adolescent psychiatrist according to the DSM-IV criteria. The patients were referred for ADHD evaluation to the psychiatric clinic of Roozbeh Hospital in Tehran, Iran. The healthy group (control group) was selected from two settings: the first and major setting was a primary school from which 50 boys were selected; and the 10 girls were selected from an all-girl's primary school. Based on the evaluation of a child and adolescent psychiatrist, none of the children in the control group had psychiatric problems. Exclusion criteria for children with ADHD and the healthy group were a history of major neurological disorders, brain injury (including epilepsy), a major medical illness, learning or verbal disability, other psychiatric disorders and the use of benzodiazepine and barbiturate drugs. All subjects were school-aged and right-handed. All procedures performed in this research were approved by the Institutional Review Board (IRB) and Ethical Committee of Tehran University of Medical Sciences (TUMS). All subjects participated in the experiment voluntarily and parents of all subjects provided informed written consent for participation in the test. The database is now available: (Ali Moti Nasrabadi, 2020).

Electroencephalogram signals were recorded by a digital device (SD-C24, Sholeh Danesh Co., Tehran, Iran) in the Psychology and Psychiatry Research Center at Roozbeh Hospital (Tehran, Iran). The EEG recording protocol was designed based on the visual attention task. Within the task, 20 images with some characters were shown to the children and they were asked to enumerate the characters. Figure 1 shows an example of a set of pictures. The sizes of the pictures were considered large enough to be easily visible and the number of the characters in each picture were chosen between 5 and 16 on a random basis. Each image was displayed immediately after the child's response in order to have continuous stimulus during the EEG recording. Thus, the child's performance defines the duration of EEG recording. Correct and incorrect answers of the participants were not considered and the task was designed without rewards. During this task, 19 electrodes (Fz, Cz, Pz, C3, T3, C4, T4, Fp1, Fp2, F3, F4, F7, F8, P3, P4, T5, T6, O1, O2) with A1 and A2 electrodes as references on earlobes were placed on the scalp based on the 10–20 system with 128 Hz sampling frequency and 16 bits EEG resolution. Electrode impedances were below 5 k Ohms.

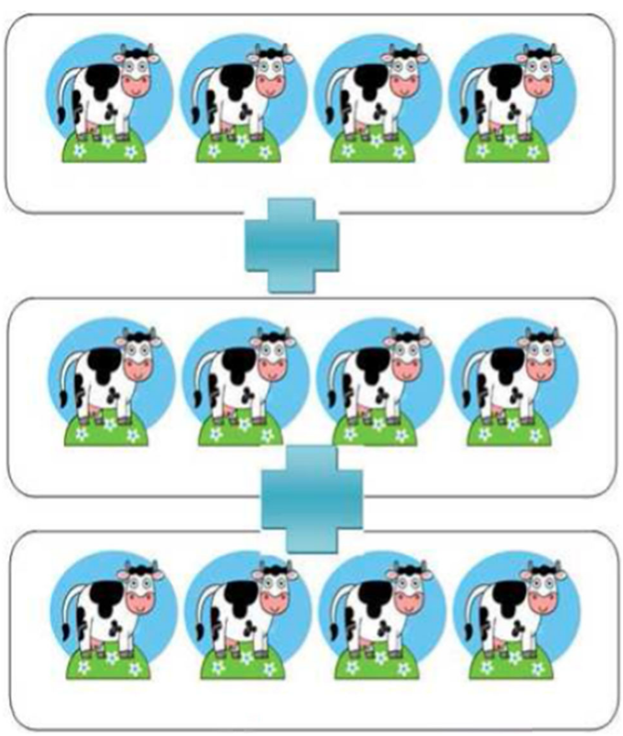

Fig. 1 The picture shown to the children as an example

Data pre-processing

EEG signals contain multiple artifacts and noise sources that must be removed before being use in analyses. The signal pre-processing method used in this work was a customized version of Makoto's pre-processing pipeline, adapted for EEGLab functions (version 14.1.1; Delorme & Makeig, 2004) running on MATLAB 2018a.

Initially, artifacts caused by eye movements and muscle activity were removed manually with visual examination. Channels that show erroneous or incorrectly acquired information were eliminated and interpolated using the signals of the adjacent channels. A band-pass FIR filter of 0.5 Hz to 48 Hz was applied to continuous EEG data in order to eliminate artifacts and was later filtered with the CleanLine plugin to remove line noise. For more artifact rejection, the EEG data was decomposed using the independent component analysis (ICA). Eye blinks and muscle artifacts were identified by brain-related independent components (ICs) and were manually removed based on their spectra, scalp maps, and time courses. After cleaning, time series were filtered in classical EEG frequency bands [delta (0.5–4 Hz), theta (4–8 Hz), alpha (8–13 Hz), beta (13–30 Hz), and lower gamma (30–45 Hz)] using FIR filter with zero phase shift that does not distort the phases. At all stages of filtering, a zero-phase Hamming-windowed filter was also provided by the firfilt-plugin distributed with EEGLab with − 6 dB cutoff frequencies. For each subject, the time series were divided into 1024 sample (8-s) segments. The number of segments varied due to different timing task for every subject. The minimum task duration was 50 s for one of the control group and the maximum task duration was 285 s for one subject with ADHD. The mean number of segments was 13.18 (std = 3.15) segments for the control group and 16.14 segments (std = 6.42) for the ADHD group.

Direction of information

PTE was used as a measure of strength and direction of information flow between EEG channels. PTE was presented by Paluš and Stefanovska (2003) and evaluated by Lobier et al. (2014). PTE is based on the same Wiener – Granger's causality principle, namely that a source signal has a causal influence on a target signal if knowing the past of both signals improves the ability to predict the target's future compared with knowing only the target's past (Granger, 1969; Wiener, 1956).

For PTE, the time series of the instantaneous phase are used as inputs of the TE function. The Hilbert transform was used to estimate the instantaneous phase time series (Rosenblum et al., 1996). Basically, TE is a specific version of the Kullback and Leibler (1951) entropy or a conditional mutual information (Hlaváčková-Schindler et al., 2007; Paluš and Stefanovska, 2003). TE can be explained in terms of the concept of uncertainty: "a source signal has a causal influence on a target signal if the uncertainty of the target signal conditioned on both its own past and that of the source signals is smaller than the uncertainty of the target signal conditioned only on its own past" (Schreiber, 2000). TE from source signal to target signal can be written as the sum of several Shannon entropies when the uncertainty or information between the source signal and the target signal at a delay δ is defined as Shannon entropy (Shannon, 1948). The TE value from source signal (X) to target signal (Y) can be expressed as

$$\mathrm{TEXY} = \sum \mathrm{p}(\mathrm{Yt} + \delta, \mathrm{Yt}, \mathrm{Xt}) \log\left(\frac{\mathrm{p}(\mathrm{Yt} + |\mathrm{Yt}, \mathrm{Xt})}{\mathrm{p}(\mathrm{Yt} + |\mathrm{Yt})}\right) \tag{1}$$

where the definition for Shannon entropy,

$$H(Y) = -\sum p(Y) \log p(Y) \tag{2}$$

was used, and the sum runs over all time steps t.

The estimation of the probabilities in Eq. (1) is time-consuming and requires fine-tuning of parameters (Wibral et al., 2011). Time series can be described in terms of their amplitudes and instantaneous phases(Rosenblum et al., 2001), following which TE can be estimated from the time series of the instantaneous phases, at low computational cost (Lobier et al., 2014; Paluš and Stefanovska, 2003). Dropping the subscript t for clarity, and to accelerate the calculations, the PTE was computed as:

$$PTEXY = \sum p(Y)p(Y)p(X) \log\left(\frac{p(Y|Y, X)}{p(Y|Y)}\right) \tag{3}$$

In Eq. (3), the probabilities are obtained by building histograms of occurrences of single, pairs, or triplets of phase estimates in an epoch (Lobier et al., 2014). Assuming that the probability distribution of source signal X is independent from that of target signal Y, Eq. (2) can be rewritten as: $\mathrm{p}(\mathrm{Y}_\delta, \mathrm{Y}, \mathrm{X}) = \mathrm{p}(\mathrm{Y}_\delta)\ \mathrm{p}(\mathrm{Y})\ \mathrm{p}(\mathrm{X})$. This assumption had no effect on the information flow patterns and could accelerate the calculation time (Prokopenko and Lizier, 2014). The number of bins in the histograms was set as $e^{0.626+0.4\ \ln(\mathrm{Ns}-\delta-1)}$ (Rosenblum et al., 2001).

The Hillbrand implementation was used to determine the prediction delay (δ) which is equal to $(\mathrm{N_s} \times \mathrm{N_{ch}})/\mathrm{N_\pm}$, with $\mathrm{N_s}$ and $\mathrm{N_{ch}}$ the number of samples and channels, respectively(Hillebrand et al., 2016). The N ± indicates the number of times the phase changes sign across time and channels. Previous results have shown that the choice of delay does not impact the results (Lobier et al., 2014). Finally, due to the lack of a meaningful upper bound for the PTE (Lobier et al., 2014) and in order to reduce biases (Hillebrand et al., 2016), normalized PTE was used:

$$\mathrm{dPTE_{xy}} = \frac{\mathrm{PTExy}}{\mathrm{PTExy} + \mathrm{PTEyx}} \tag{4}$$

$\mathrm{dPTE_{xy}}$ range is between 0 and 1. When information flows preferentially from X to Y, $0.5 < \mathrm{dPTE_{xy}} \leq 1$. When information flows preferentially towards X from Y, $0 \leq \mathrm{dPTE_{xy}} < 0.5$. The dPTE value was computed for all pairwise channels, forming a dPTE matrix for every segment in each frequency band for all the subjects. Subsequently, for each frequency band, the computed dPTE values for all segments were averaged over segments to compute one average dPTE value per subject. Thus, there is one square dPTE matrix, defined as mean dPTE, for each subject with rows and columns by the number of EEG channels. The regional dPTE values were computed by averaging all pairwise mean dPTE values from one channel to all the other channels, and one regional dPTE value was obtained for every of 19 channels in each frequency band. The regional dPTE values indicate that a brain area is a driver (0.5 < regional dPTE ≤ 1) or a receiver (0 ≤ regional dPTE < 0.5), relative to other areas.

To establish whether there are consistent patterns of information flow, usually a posterior-anterior index (PAx) (Engels et al., 2017; Hillebrand et al., 2016) was calculated for each frequency band. In addition to PAx, IAx, IPx and LRx indices are introduced as follows:

$$\begin{aligned} IAx &= \{dPTE\}_{anterior} \\ IPx &= \{dPTE\}_{posterior} \\ PAx &= \{dPTE\}_{posterior} - \{dPTE\}_{anterior} \\ LRx &= \{dPTE\}_{left} - \{dPTE\}_{right} \end{aligned} \tag{5}$$

where the dPTE was averaged over a set of anterior, posterior, left, and right regions, respectively. Table 1 indicates the channels for each region. To investigate whether there are different information flows in anterior or posterior brain regions between ADHD and control subjects, the

Table 1 Specify channels to relevant regions

Region	Channel
Anterior	Fp1, Fp2, F7, F3, Fz, F4, F8
Posterior	T5, P3, Pz, P4, T6, O1, O2
Left	Fp1, F3, F7, C3, T3, T5, P3, O1
Right	Fp2, F4, F8, C4, T4, T6, P4, O2

internal-anterior (IAx) and internal-posterior (IPx) indices were computed, respectively. To calculate each of those indices for every individual, only the dPTE values associated with the connections that existed in that region were averaged. A positive and a negative PAx indicates posterior to anterior and anterior to posterior information flow respectively. In the same way, a positive LRx indicates left-to-right information flow, and a negative LRx indicates right-to-left information flow.

Statistical analysis

For each frequency band separately, non-parametric permutation tests were used to compare group-level 19 regional dPTE values in each channel between the two groups. Statistical testing was performed according to the following steps:

1. Averaging the regional dPTE values for ADHD and control groups overall subjects of every group;
2. Computing the observed absolute difference between the group-level regional dPTEs of ADHD, and control group;
3. Permuting the group assignments of the individuals' regional dPTE values for ADHD and control groups;
4. Repeating steps 1 to 3 to obtain 5,000 permutations of absolute differences for ADHD and control groups.

To obtain a p-value, the observed absolute difference was tested against the sampled distribution. The false discovery rate (FDR) correction was used to correct p-values of pairwise comparisons (Benjamini and Hochberg, 1995) and to control the proportion of type I errors. The FDR-corrected p-values were considered to be significant at < 0.05.

These analyses were repeated for the individual mean dPTE values between all pairs of EEG channels (i.e. the individual mean dPTE values, instead of the regional dPTE values). Afterward, directed differential connectivity graphs (dDCGs) were constructed to characterize the significant changes in dPTE between the two groups. The observed value of each index was computed for the averaged dPTE values in each subject. Each index in each frequency band was normalized by the absolute maximum value that could have been obtained with the dPTE values for these individual channels. The significance of group differences in each index was assessed using randomization testing (with the same parameters as before), where the average dPTE values were permuted across the channels, after which the index was computed.

Results

Information flow between regions

First, the regional dPTE per EEG channel was examined in each frequency band in two groups. Figure 2 displays the average information flow between a single region and all other regions to estimate the preferred direction of information flow (outgoing or incoming) for each region in the ADHD and control groups.

According to Fig. 2, in the delta band, occipital channels in ADHDs were more driving compared to occipital channels in the control group relatively. In both groups, while the frontal lobe acts as the receiver of information, the left temporal lobes of the control subjects shows more outgoing information flow than the ADHD subjects. In the theta band, occipital channels in the control subjects were more driving and are supposed to be a path of information from the posterior region to the parietal and anterior parts of the brain, while in ADHD subjects, this direction is from anterior to posterior regions. In the beta band, more areas in the front and center of the brain in the control group act as transmitters of information compared to the ADHD subjects. Figure 3 represents channels that demonstrated a significant between-group difference in mean regional dPTE in each frequency band by group-level permutation tests with a FDR correction (p-value < 0.05). Red and blue dots indicate whether the mean regional dPTE was significantly higher or lower in controls than in ADHD patients, respectively. Below each image, the value of the regional dPTE is written for channels with significant differences for the two groups.

The calculations for the introduced indices show that the theta band was the only frequency band showing differences in PAx between patients and controls. As shown in Fig. 2, in the theta band there is a dominant pattern of posterior-to-anterior information flow for the healthy controls. In ADHD patients, the posterior-to-anterior pattern was disrupted. It was also quantified by the significantly lower (p-value = 0.037) PAx in ADHD patients (PAx = −0.0801) compared to healthy controls (PAx = 0.0610). In the delta frequency band, IAx shows that controls (IAx = 0.9905) have a less internal anterior information flow (P-value = 0.002) in comparison with ADHD patients

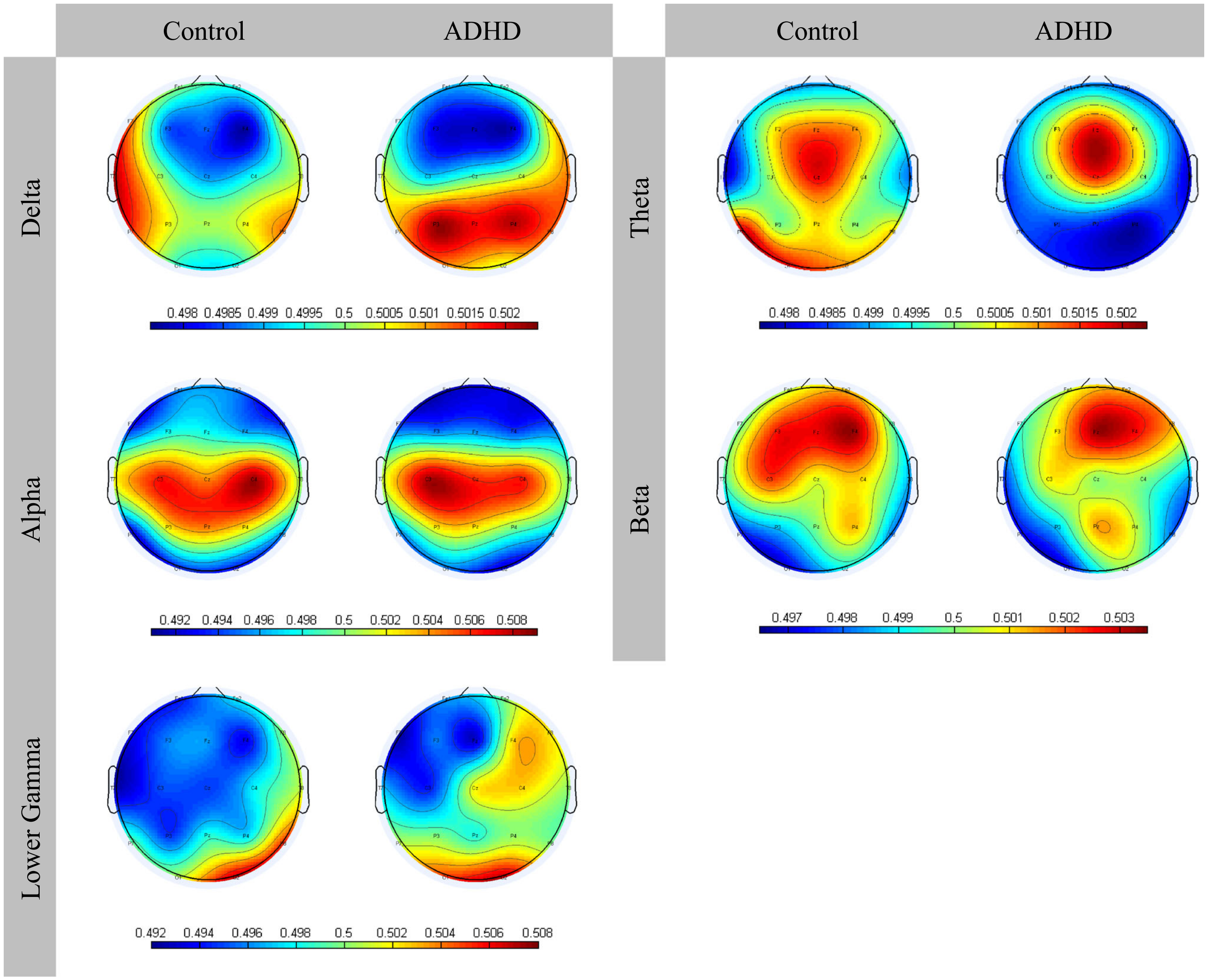

Fig. 2 Mean dPTE for each regional (Regional dPTE) displayed as a color-coded map. Red and Blue color indicate information outflow and inflow respectively. The differences in posterior region in Delta and Theta frequency band and in anterior region in Beta frequency band between Control and ADHD subjects are noticeable

(IAx = 0.9931). In the beta frequency band, however, controls (IAx = 0.9980) have a more internal anterior information flow (p-value = 0.002) in comparison with ADHD patients (IAx = 0.9945). IPx in the theta band indicates (p-value = 0.002) less local patterns of internal information flow in the controls (IPx = 0.9926) as compared with the ADHD subjects (IPx = 0.9950) in the posterior region. The results of the LRx in all frequency bands and IAx and IPx in the alpha and lower gamma bands did not show a significant difference between the two groups.

Information flow between channels

Figure 4 shows the mean dPTE matrices in the beta band for the controls and ADHD subjects. These figures clearly display that the mean dPTE values for the ADHD patients show less variation and are more centered on the equilibrium value of 0.5, i.e. no preferred direction of information flow, compared to the controls.

The significant differences ($p < 0.05$) in directed connections (mean dPTE) between pairwise channels in controls and ADHD subjects are shown in Fig. 5a for the theta and Fig. 5b for the beta bands. In this figure, the red and blue colors indicate whether the strength of information flow between pairs of brain channels was significantly higher or lower in the controls than in the ADHD patients, respectively. Green cells are connections that demonstrate no difference in statistical testing.

For visualization, dDCGs between two groups in the theta and beta frequency band are shown in Fig. 6. Similar to other figures, red and blue lines indicate whether the strength of dPTE values between pairs of brain channels is

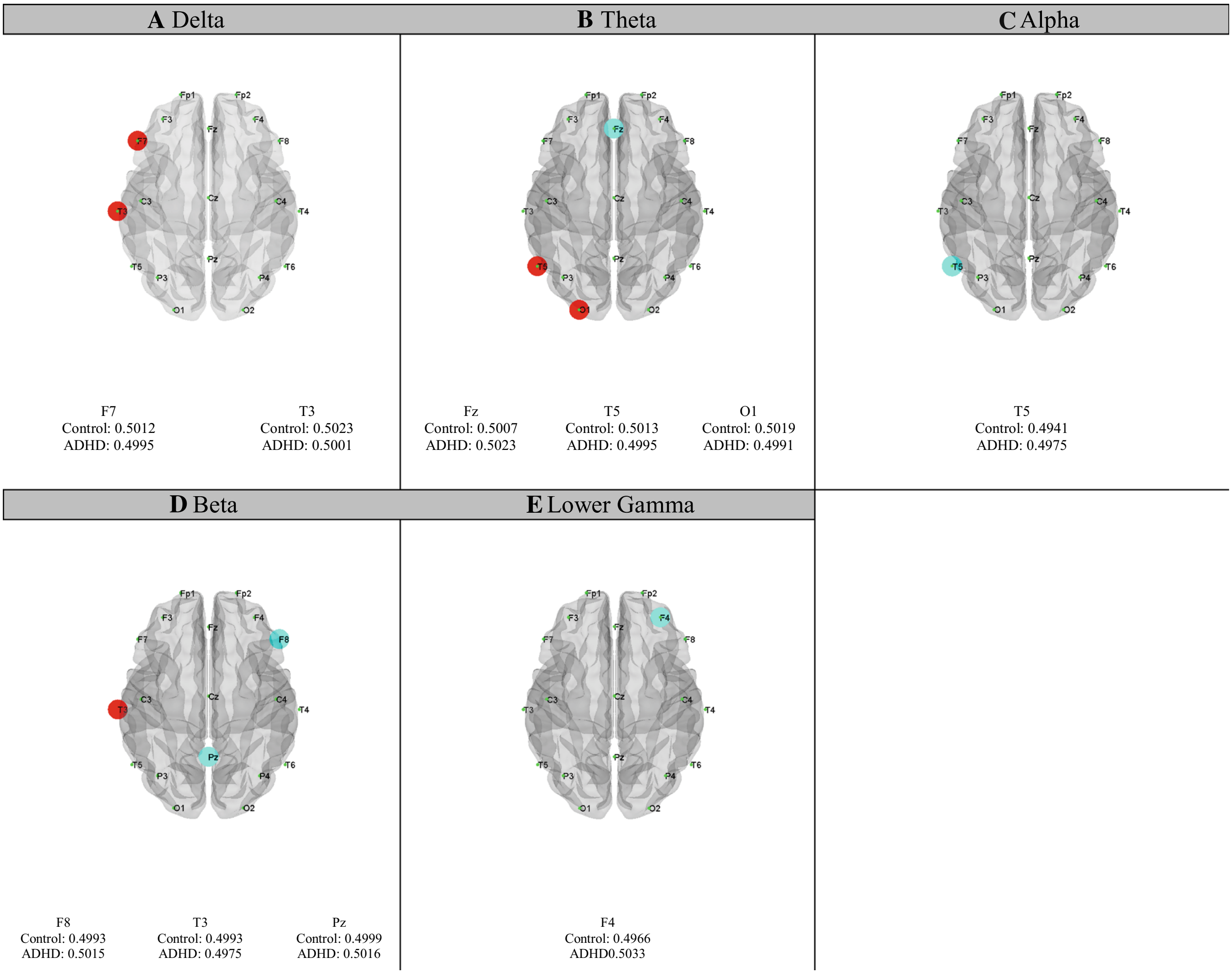

Fig. 3 **a-e** Cortical surface representation channels that demonstrate significant between-group difference in Regional dPTE in each frequency band; Red and Blue color indicate whether the mean regional dPTE was significantly higher or lower in control than ADHD patients, respectively. Regional dPTE for channels in grey were not significantly different between two groups

significantly higher or lower in the controls than in the ADHD subjects, respectively.

Figure 6a shows that the information flow between posterior regions and frontal regions was decreased in ADHD subjects in the theta band. Furthermore, there are information flows from anterior to posterior region in patients. Interestingly, the largest number of different pathways between the two groups in the theta band are in the left hemisphere of the brain. In the beta band (Fig. 6b), significant connections with higher dPTE values in the control group were located mostly in frontal regions and related to internal anterior connection. In particular, the connections between the electrodes of the frontal region for the F8 electrode are among the information paths in which there are significant differences between the two groups. A similar pattern is evident in the Pz electrode area in the posterior region of the brain.

Discussion

In this study, it was hypothesized that the flow of information in the brains of children with ADHD is different from that in healthy children. Using the EEG data collected during the visual attention task for the two groups of subjects, this hypothesis was studied utilizing the dPTE as a measure of the direction of information flow and effective connectivity. The hypothesis was confirmed for the delta, theta, and beta bands with specific indices. The main finding of this study is the higher information flow in the theta band from the posterior to the anterior and in the internal anterior region in the beta band in the control group than in the ADHD subjects.

According to Wibral (Wibral et al., 2011, 2014), the TE-based measures represent the amount of predictive information transfer between two processes and increasing the

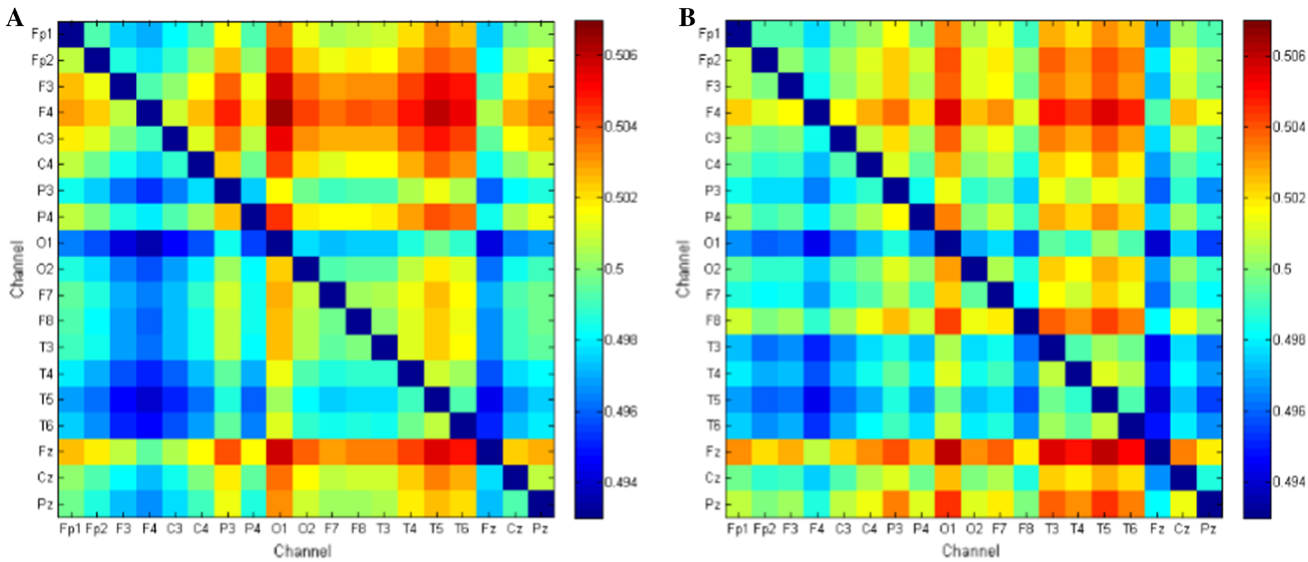

Fig. 4 Direction of information flow patterns in the beta band. Mean dPTE matrices for Controls **a** and ADHDs **b**

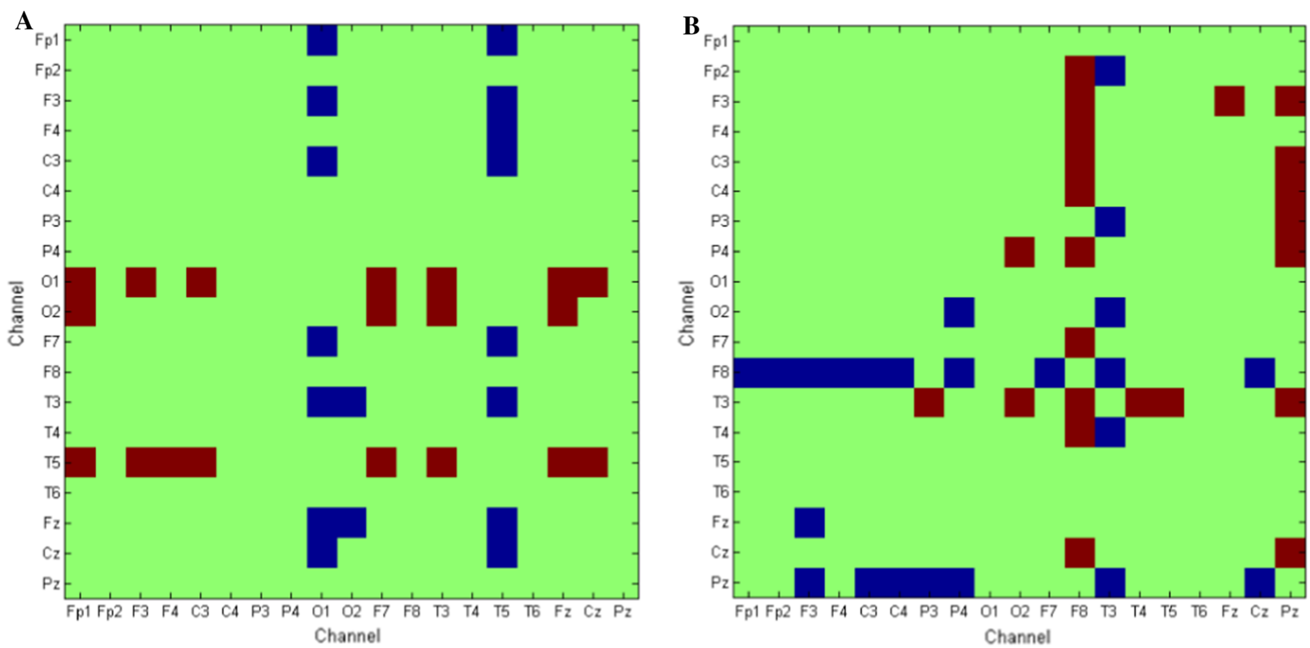

Fig. 5 *P*-value ($p < 0.05$) matrices for each channel showing between -group differences in directed connection between pairwise channel; Permutation test with FDR correction. Red and blue colors indicate whether the strength of dPTE values between pairs of brain channels significantly higher or lower in control than ADHD, respectively. **a** is p-value matrix for theta and **b** is for beta band

strength of interaction may lead to identical copies of the dynamics, it also reduces the possibility of information transfer between them. In this case, the TE-based measures show a smaller value than the cases with a smaller coupling strength and incomplete synchronization. Simply, there is indeed no information transfer without a causal interaction, but the reverse does not hold. In fact, not all causal interactions serve the purpose of information transfer. In a complete synchronization interaction, there is a causal interaction between the two systems, but no information transfer (TE = 0). Thus, the interpretation of causality must be proceeded carefully and we insist on using information direction phrase instead of causal effect size in analyzing dPTE results. Since dPTE does not require a model for interactions and is inherently nonlinear, and uses the instantaneous phases of signals to determine connectivity, it can overcome the limitation of linear mixing and volume conduction. Low computational cost is another feature of the dPTE measure, while dPTE (or TE) like any other bivariate measure it may be affected by indirect

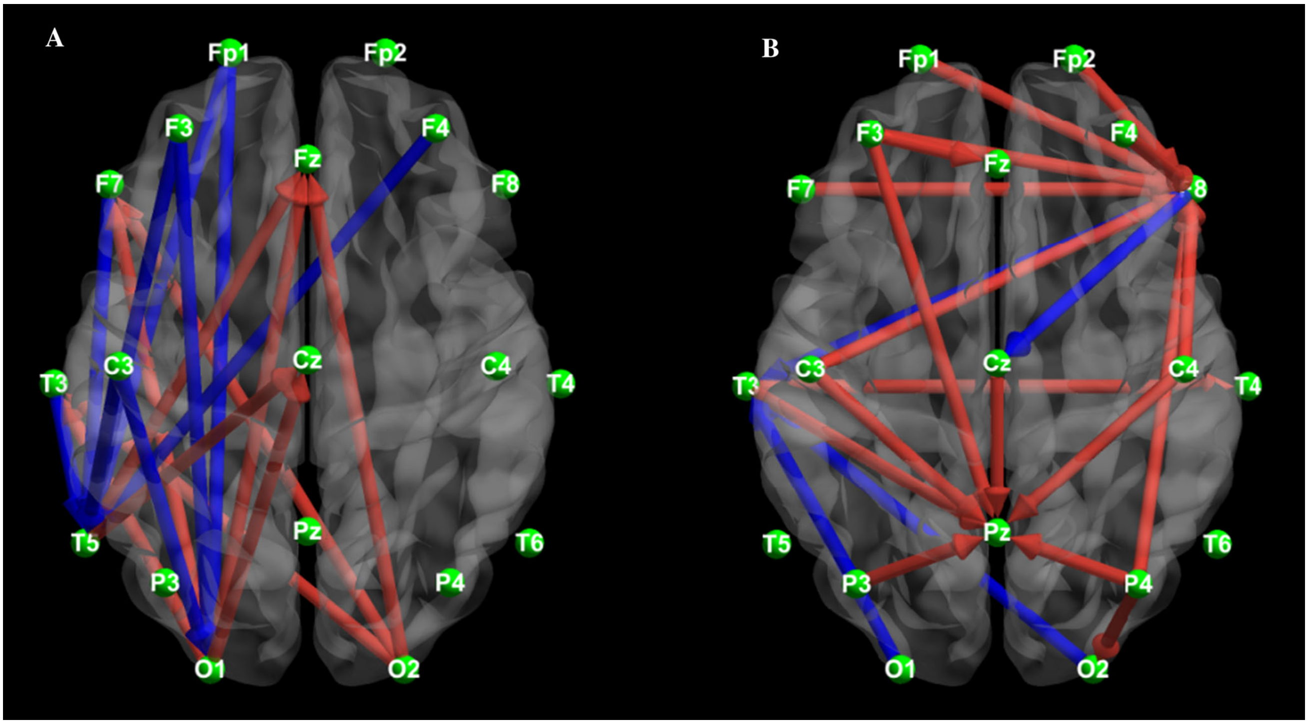

Fig. 6 dDCG between ADHD patients and controls in theta band **a** and beta band **b** are shown by using BrainNet Viewer

connectivity (Ursino et al., 2020). In general, dPTE (and TE) can be a proper measure for determining the direction of information transfer in brain regions (Lobier et al., 2014; Wibral et al., 2011).

This study used the PAx index to determine the consistent patterns of information flow from the posterior to the anterior areas in each frequency band. The statistical test in the theta band showed a significant difference in the information flow from the posterior to the anterior region between the two groups. The negative value of the average PAx in patients indicates the information flow from the anterior to the posterior regions, while the positive value of the average PAx in the control group shows the flow of information from the posterior to the anterior regions. Our results using the PAx complement the results of a previous study on functional disconnection between the frontal and occipital regions of the brain in ADHD subjects (Mazaheri et al., 2010). Thus, this disconnection in our research showed itself in the theta frequency band in ADHD group. Figure 3 shows that the significant difference between the two groups in the regional dPTE values is related to T5 and O1 electrodes, and was not only higher in the control group, but also greater than 0.5 (outward information flow). In the ADHD group, however, it was less than 0.5 (inward information flow). Thus, it can be concluded that the temporal and occipital lobes in the left hemisphere of the brain in the control group play a greater role in sending information to other areas of the brain compared to the ADHD group in the theta frequency band. The Fz electrode plays the role of outward information flow in both groups. Moreover, it is more dPTE in the ADHD subjects. The results of pairwise channels dPTE values (Fig. 6a) indicates higher connections reaching this channel from the posterior region with a lower amount of regional dPTE for healthy children. These values confirm the results of the PAx in the theta band. The PAx index in the other frequency bands did not report a significant difference between the two groups.

This study introduces two indices, IAx and IPx to determine the strength of internal communications in the anterior and posterior regions, respectively. The results of the statistical test with the IAx index in the delta band show a significantly higher strength of interactions in the anterior region of the ADHD subjects than in the healthy individuals. Figures 2 and 3 show that the temporal-frontal region of healthy individuals in the delta band in the left hemisphere of the brain has more strength to transmit information. This result, together with the IAx results in the delta band, showed that the F7 and T3 electrode regions in the control group send stronger information to the central regions of the brain (not the anterior regions) than in the ADHD group. This result was confirmed in dDCG analysis between the two groups. The IPx results in the theta band are in line with the PAx results. IPx showed that the strength of intra-regional communication is higher in ADHD group in the posterior of the brain, and thus the connectivity from posterior to anterior of the brain in this group is less than that in the control group in the theta band. The results of other studies on functional connectivity (Ahmadlou and Adeli, 2010; 2011a) show a significant difference between the two groups in the T5 and O2 electrodes in the delta and theta bands respectively. As mentioned in our study, the between-group differences in the regional dPTE values occur in the T3 (in delta band) and in T5 and O1 (in the theta band). It can be claimed that these two results are related to each other due to the electrode's location and the frequency bands which are close to each other.

The results of statistical tests on the IAx index in the beta band showed that intra-regional connectivity in the anterior regions of the brain is significantly higher in the control group than in the ADHD group. Previous studies by fMRI found abnormalities in the lateral inferior prefrontal cortex on the right hemisphere (Booth et al., 2005; Rubia et al., 2010, 2009b) and indicate evidence for a reduced frontoparietal functional connectivity in children with ADHD (Kelly et al., 2007). Studies have shown a reduced inter-connectivity between the key areas of attention that are also the key regions of dysfunction in the ADHD children, between the right inferior prefrontal cortex, basal ganglia, the parietal lobes, and the cerebellum. Although they demonstrate that the dysfunctions in children with ADHD are not restricted to the isolated brain regions, they compromise the functional inter-regional connectivity between these areas (Rubia et al., 2009a). Additionally, the orbitofrontal cortex (involved in salience attribution) in the ADHD children had lower connectivity with the superior parietal cortex (involved in attention processing) (Tomasi and Volkow, 2012). Our findings are consistent with previous reports and also provide new implications for understanding the information flow that reduces the connectivity in the prefrontal cortex in ADHD children with the results of IAx. In addition, the reduced connectivity from the frontal region to another region occurred in the beta frequency band, specifically related to the right side of the frontal region through the F8 electrode (Fig. 6b). In this figure, it is clear that most of the connections that are made from the front electrodes to the F8 electrode are statistically different in terms of information transfer between the two groups. In all of these connectivities, the average amount of dPTE in the healthy group is higher. Therefore, the lower amount of regional dPTE in the F8 electrode in the control group indicates that it has a more receptive role in transmitting information in comparison with the ADHD group. This result is evident in the study of dPTE values between pairwise channels in both groups. Our results using the IAx confirm the basic research with EEGs stating that ADHD subjects have a decreased absolute and/or relative beta power in frontal regions in comparison with the age-matched healthy subjects (Barry and Clarke, 2013; Barry et al., 2003; Lenartowicz and Loo, 2014; Monastra, 2008). The connections that reach the Pz-electrode from the lateral parietal regions (P3 and P4) and the central regions (C3, Cz and C4) are significantly stronger in the healthy individuals in the beta band. Compared to the theta band, where different connections between the two groups occurred long-distance, in the beta band, these statistical differences occur in electrodes with a short distance from each other. The alpha and lower gamma frequency bands, although there are channels (T5 and F4) reporting significant differences in regional dPTE values between the two groups, were not examined, as they did not show a statistical difference with the indices.

Conclusion

In conclusion, this study shows that the posterior to anterior pattern of connectivity commonly seen in the control group is disturbed in the ADHD patients in the theta band during visual task. Also in the beta band, the information flow in the pathways between the anterior regions was significantly higher in the control group with the statistical permutation test. This difference is highlighted in the area related to the right frontal brain regions (particularly F8 electrode) that play important roles in the attention process. In this frequency band, the connections that reach Pz from the lateral parietal and central regions are significantly stronger in the healthy individuals in comparison with the ADHD subjects. The results of statistical testing on the internal connections in the delta band in the anterior region show that the strength of these connections in ADHD subjects is significantly higher. The obtained results provide an understanding of differences in the information flow of the brain in the ADHD children in comparison with the healthy children.

References

Ahmadlou M, Adeli H (2010) Wavelet-synchronization methodology: a new approach for EEG-based diagnosis of ADHD. Clin EEG Neurosci 41:1–10. https://doi.org/10.1177/155005941004100103

Ahmadlou M, Adeli H (2011a) Functional community analysis of brain: a new approach for EEG-based investigation of the brain pathology. Neuroimage 58:401–408. https://doi.org/10.1016/j.neuroimage.2011.04.070

Ahmadlou M, Adeli H (2011b) Fuzzy synchronization likelihood with application to attention-deficit/hyperactivity disorder. Clin EEG Neurosci 42:6–13. https://doi.org/10.1177/155005941104200105

Allahverdy A, Moghadam AK, Mohammadi MR, Nasrabadi AM (2016) Detecting ADHD children using the attention continuity as nonlinear feature of EEG. Front Biomed Technol 3:28–33

Barry RJ, Clarke AR (2013) Resting state brain oscillations and symptom profiles in attention deficit/hyperactivity disorder.

Suppl Clin Neurophysiol 62:275–287. https://doi.org/10.1016/B978-0-7020-5307-8.00017-X

Barry RJ, Clarke AR, Johnstone SJ (2003) A review of electrophysiology in attention-deficit/hyperactivity disorder: I qualitative and quantitative electroencephalography. Clin Neurophysiol 114:171–183. https://doi.org/10.1016/s1388-2457(02)00362-0

Başar E, Güntekin B (2013) Review of delta, theta, alpha, beta, and gamma response oscillations in neuropsychiatric disorders. Suppl Clin Neurophysiol 62:303–341. https://doi.org/10.1016/B978-0-7020-5307-8.00019-3

Benjamini Y, Hochberg Y (1995) Controlling the false discovery rate: a practical and powerful approach to multiple testing. J Royal Stat Soc: series B (Methodol) 57:289–300. https://doi.org/10.1111/j.2517-6161.1995.tb02031.x

Boon LI, Hillebrand A, Dubbelink KTO, Stam CJ, Berendse HW (2017) Changes in resting-state directed connectivity in cortico-subcortical networks correlate with cognitive function in Parkinson's disease. Clin Neurophysiol 128:1319–1326

Booth JR, Burman DD, Meyer JR, Lei Z, Trommer BL, Davenport ND, Li W, Parrish TB, Gitelman DR, Marsel Mesulam M (2005) Larger deficits in brain networks for response inhibition than for visual selective attention in attention deficit hyperactivity disorder (ADHD). J Child Psychol Psychiatry 46:94–111. https://doi.org/10.1111/j.1469-7610.2004.00337.x

Clarke AR, Barry RJ, McCarthy R, Selikowitz M, Johnstone SJ, Hsu CI, Magee CA, Lawrence CA, Croft RJ (2007) Coherence in children with attention-deficit/hyperactivity disorder and excess beta activity in their EEG. Clin Neurophysiol 118:1472–1479. https://doi.org/10.1016/j.clinph.2007.04.006

Dauwan M, van Dellen E, van Boxtel L, van Straaten ECW, de Waal H, Lemstra AW, Gouw AA, van der Flier WM, Scheltens P, Sommer IE, Stam CJ (2016) EEG-directed connectivity from posterior brain regions is decreased in dementia with Lewy bodies: a comparison with Alzheimer's disease and controls. Neurobiol Aging 41:122–129. https://doi.org/10.1016/j.neurobiolaging.2016.02.017

Engels MMA, Yu M, Stam CJ, Gouw AA, van der Flier WM, Scheltens P, van Straaten ECW, Hillebrand A (2017) Directional information flow in patients with Alzheimer's disease. A source-space resting-state MEG study. Neuroimage Clin 15:673–681. https://doi.org/10.1016/j.nicl.2017.06.025

González JJ, Alba G, Mañas S, González A, Pereda E (2017) Assessment of ADHD through electroencephalographic measures of functional connectivity. ADHD-New Dir Diagn Treat: https://doi.org/10.5772/60559

Granger CW (1969) Investigating causal relations by econometric models and cross-spectral method Econometrica. J Econom Soc. https://doi.org/10.2307/1912791

Hasanzadeh F, Mohebbi M, Rostami R (2020) Graph theory analysis of directed functional brain networks in major depressive disorder based on EEG signal. J Neural Eng 17:026010. https://doi.org/10.1088/1741-2552/ab7613

Hillebrand A, Tewarie P, Van Dellen E, Yu M, Carbo EW, Douw L, Gouw AA, Van Straaten EC, Stam CJ (2016) Direction of information flow in large-scale resting-state networks is frequency-dependent. Proc Natl Acad Sci 113:3867–3872. https://doi.org/10.1073/pnas.1515657113

Hlaváčková-Schindler K, Paluš M, Vejmelka M, Bhattacharya J (2007) Causality detection based on information-theoretic approaches in time series analysis. Phys Rep 441:1–46. https://doi.org/10.1016/j.physrep.2006.12.004

Kelly AM, Margulies DS, Castellanos FX (2007) Recent advances in structural and functional brain imaging studies of attention-deficit/hyperactivity disorder. Curr Psychiatry Rep 9:401–407. https://doi.org/10.1007/s11920-007-0052-4

Kessler RC, Adler LA, Berglund P, Green JG, McLaughlin KA, Fayyad J, Russo LJ, Sampson NA, Shahly V, Zaslavsky AM (2014) The effects of temporally secondary co-morbid mental disorders on the associations of DSM-IV ADHD with adverse outcomes in the US National Comorbidity Survey Replication Adolescent Supplement (NCS-A). Psychol Med 44:1779–1792. https://doi.org/10.1017/S0033291713002419

Kiiski H, Rueda-Delgado LM, Bennett M, Knight R, Rai L, Roddy D, Grogan K, Bramham J, Kelly C, Whelan R (2020) Functional EEG connectivity is a neuromarker for adult attention deficit hyperactivity disorder symptoms. Clin Neurophysiol 131:330–342. https://doi.org/10.1016/j.clinph.2019.08.010

Kooij SJ, Bejerot S, Blackwell A, Caci H, Casas-Brugue M, Carpentier PJ, Edvinsson D, Fayyad J, Foeken K, Fitzgerald M, Gaillac V, Ginsberg Y, Henry C, Krause J, Lensing MB, Manor I, Niederhofer H, Nunes-Filipe C, Ohlmeier MD, Oswald P, Pallanti S, Pehlivanidis A, Ramos-Quiroga JA, Rastam M, Ryffel-Rawak D, Stes S, Asherson P (2010) European consensus statement on diagnosis and treatment of adult ADHD: the European Network Adult ADHD. BMC Psychiatry 10:67. https://doi.org/10.1186/1471-244X-10-67

Kullback S, Leibler RA (1951) On information and sufficiency. Ann Math Stat 22:79–86. https://doi.org/10.2307/2236703

Lenartowicz A, Loo SK (2014) Use of EEG to diagnose ADHD. Current Psychiatry Rep 16:498. https://doi.org/10.1007/s11920-014-0498-0

Lobier M, Siebenhuhner F, Palva S, Palva JM (2014) Phase transfer entropy: a novel phase-based measure for directed connectivity in networks coupled by oscillatory interactions. Neuroimage 85(2):853–872. https://doi.org/10.1016/j.neuroimage.2013.08.056

Mazaheri A, Coffey-Corina S, Mangun GR, Bekker EM, Berry AS, Corbett BA (2010) Functional disconnection of frontal cortex and visual cortex in attention-deficit/hyperactivity disorder. Biol Psychiatry 67:617–623. https://doi.org/10.1016/j.biopsych.2009.11.022

Mohammadi MR, Khaleghi A, Nasrabadi AM, Rafieivand S, Begol M, Zarafshan H (2016) EEG classification of ADHD and normal children using non-linear features and neural network. Biomed Eng Lett 6:66–73. https://doi.org/10.1007/s13534-016-0218-2

Monastra VJ (2008) Quantitative electroencephalography and attention-deficit/hyperactivity disorder: implications for clinical practice. Curr Psychiatry Rep 10:432–438. https://doi.org/10.1007/s11920-008-0069-3

Nasrabadi AM, Allahverdy A, Samavati M, Mohammadi MR (2020) EEG data for ADHD / Control children. https://doi.org/10.21227/rzfh-zn36

Paluš M, Stefanovska A (2003) Direction of coupling from phases of interacting oscillators: an information-theoretic approach. Phys Rev E 67:055201. https://doi.org/10.1103/PhysRevE.67.055201

Prokopenko M, Lizier JT (2014) Transfer entropy and transient limits of computation. Sci Rep 4:5394. https://doi.org/10.1038/srep05394

Pub AP (2013) Diagnostic and statistical manual of mental disorders (DSM-5®). Am Psychiatric Pub. https://doi.org/10.1176/appi.books.9780890425596

Rosenblum M, Pikovsky A, Kurths J, Schäfer C, Tass PA (2001) Phase synchronization: from theory to data analysis. Handb Biol Phys 4:93–94

Rosenblum MG, Pikovsky AS, Kurths J (1996) Phase synchronization of chaotic oscillators. Phys Rev Lett 76:1804–1807. https://doi.org/10.1103/PhysRevLett.76.1804

Rubia K, Cubillo A, Smith AB, Woolley J, Heyman I, Brammer MJ (2010) Disorder-specific dysfunction in right inferior prefrontal cortex during two inhibition tasks in boys with attention-deficit hyperactivity disorder compared to boys with obsessive–

compulsive disorder. Human Brain Mapp 31:287–299. https://doi.org/10.1002/hbm.20864

Rubia K, Halari R, Cubillo A, Mohammad AM, Brammer M, Taylor E (2009a) Methylphenidate normalises activation and functional connectivity deficits in attention and motivation networks in medication-naive children with ADHD during a rewarded continuous performance task. Neuropharmacology 57:640–652. https://doi.org/10.1016/j.neuropharm.2009.08.013

Rubia K, Halari R, Smith AB, Mohammad M, Scott S, Brammer MJ (2009b) Shared and disorder-specific prefrontal abnormalities in boys with pure attention-deficit/hyperactivity disorder compared to boys with pure CD during interference inhibition and attention allocation. J Child Psychol Psychiatry 50:669–678. https://doi.org/10.1111/j.1469-7610.2008.02022.x

Schreiber T (2000) Measuring information transfer. Phys Rev Lett 85:461–464. https://doi.org/10.1103/PhysRevLett.85.461

Shannon CE (1948) A mathematical theory of communication. Bell Syst Tech J 27:379–423

Tomasi D, Volkow ND (2012) Abnormal functional connectivity in children with attention-deficit/hyperactivity disorder. Biol Psychiatry 71:443–450. https://doi.org/10.1016/j.biopsych.2011.11.003

Ursino M, Ricci G, Magosso E (2020) Transfer entropy as a measure of brain connectivity: a critical analysis with the help of neural mass models. Front Comput Neurosci. https://doi.org/10.3389/fncom.2020.00045

van den Heuvel MP, Sporns O (2013) Network hubs in the human brain. Trends Cogn Sci 17:683–696. https://doi.org/10.1016/j.tics.2013.09.012

van Diessen E, Numan T, van Dellen E, van der Kooi AW, Boersma M, Hofman D, van Lutterveld R, van Dijk BW, van Straaten EC, Hillebrand A, Stam CJ (2015) Opportunities and methodological challenges in EEG and MEG resting state functional brain network research. Clin Neurophysiol 126:1468–1481. https://doi.org/10.1016/j.clinph.2014.11.018

Vinck M, Oostenveld R, van Wingerden M, Battaglia F, Pennartz CM (2011) An improved index of phase-synchronization for electrophysiological data in the presence of volume-conduction, noise and sample-size bias. Neuroimage 55:1548–1565. https://doi.org/10.1016/j.neuroimage.2011.01.055

Wang J, Wang J, Sun J, Tong S, Hong X (2019) Phase Transfer Entropy between Frontal and Posterior Regions during Visual Spatial Attention. In: 2019 9th International IEEE/EMBS Conference on Neural Engineering (NER). https://doi.org/10.1109/NER.2019.8717130

Wibral M, Rahm B, Rieder M, Lindner M, Vicente R, Kaiser J (2011) Transfer entropy in magnetoencephalographic data: quantifying information flow in cortical and cerebellar networks. Prog Biophys Mol Biol 105:80–97. https://doi.org/10.1016/j.pbiomolbio.2010.11.006

Wibral M, Vicente R, Lindner M (2014) Transfer entropy in neuroscience, in *Directed information measures in neuroscience*. Springer, NewYork

Wiener N (1956) The theory of prediction. Modern mathematics for engineers, New York